Karlsruhe Institute of Technology

Institute for Applied Materials

Plasticity

Lecture for “Mechanical Engineering” and “Materials Science and Engineering”
Dr.-Ing. Alexander Kauffmann (Bldg. 10.91, R. 375)
Prof. Martin Heilmaier (Bldg. 10.91, R. 036)

Version 22-02-21

Institute for Applied Materials (IAM-WK)

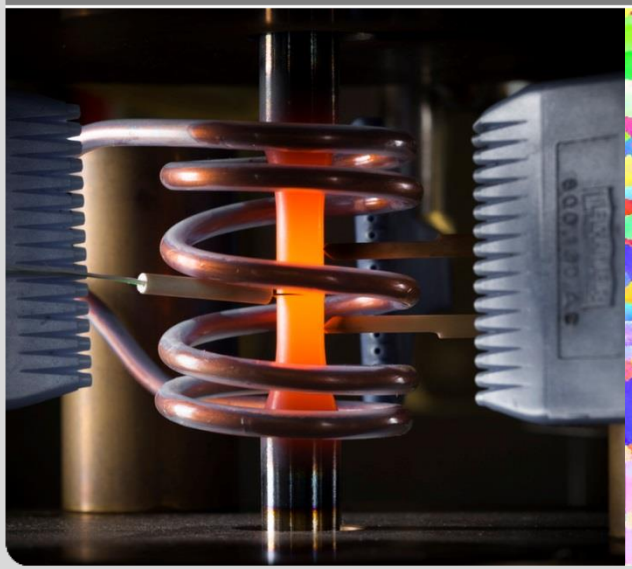

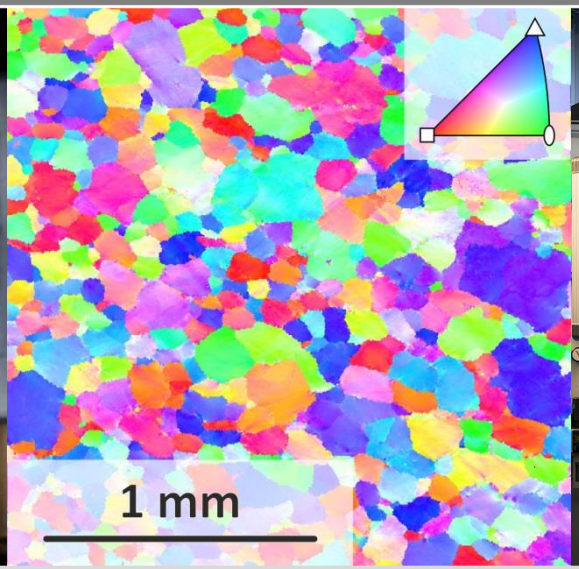

Topics

- Observation of Dislocations
  - Transmission Electron Microscopy
  - Scanning Electron Microscopy
  - Field Ion Microscopy (only for notice)
  - Etch Pits
  - Electrical Resistivity
  - X-ray Diffraction

Transmission Electron Microscopy (TEM)

- **Direct evidence** for dislocations is possible.
- **Electrons transmit thin samples** of about 50 to 200 nm in thickness.
- **Different types of contrast** are possible:
  - Imaging of **displaced atomic columns in high-resolution** images
  - Imaging of **altered diffraction conditions in the vicinity of dislocations**

Transmission Electron Microscopy (TEM)

electron gun and condenser lenses

sample

objective lens

back focal plane

intermediate image

intermediate lens

intermediate image

projector lens

image or diffraction pattern

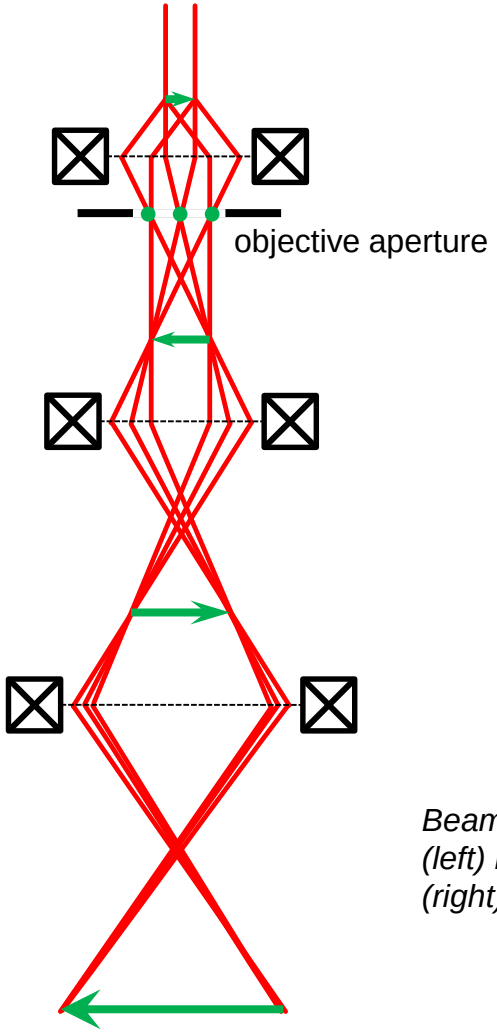

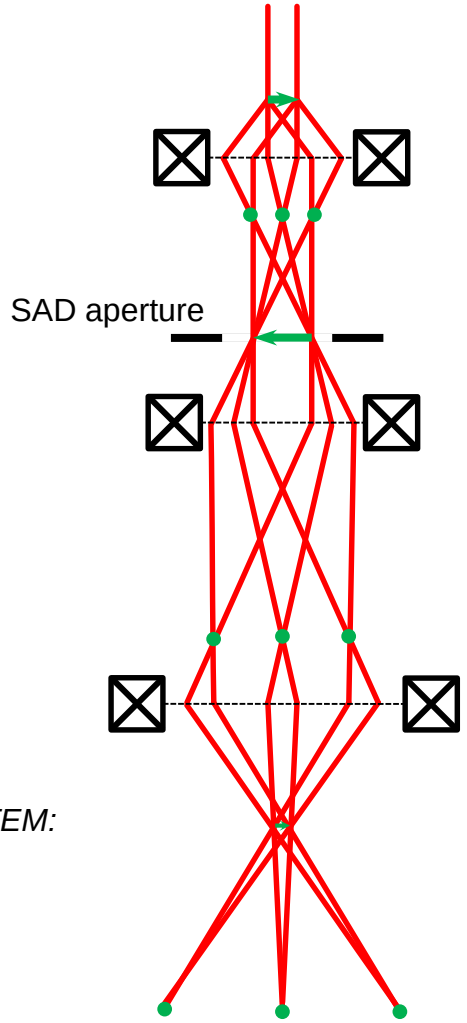

Beam path in the TEM:
(left) imaging
(right) diffraction

Transmission Electron Microscopy (TEM)

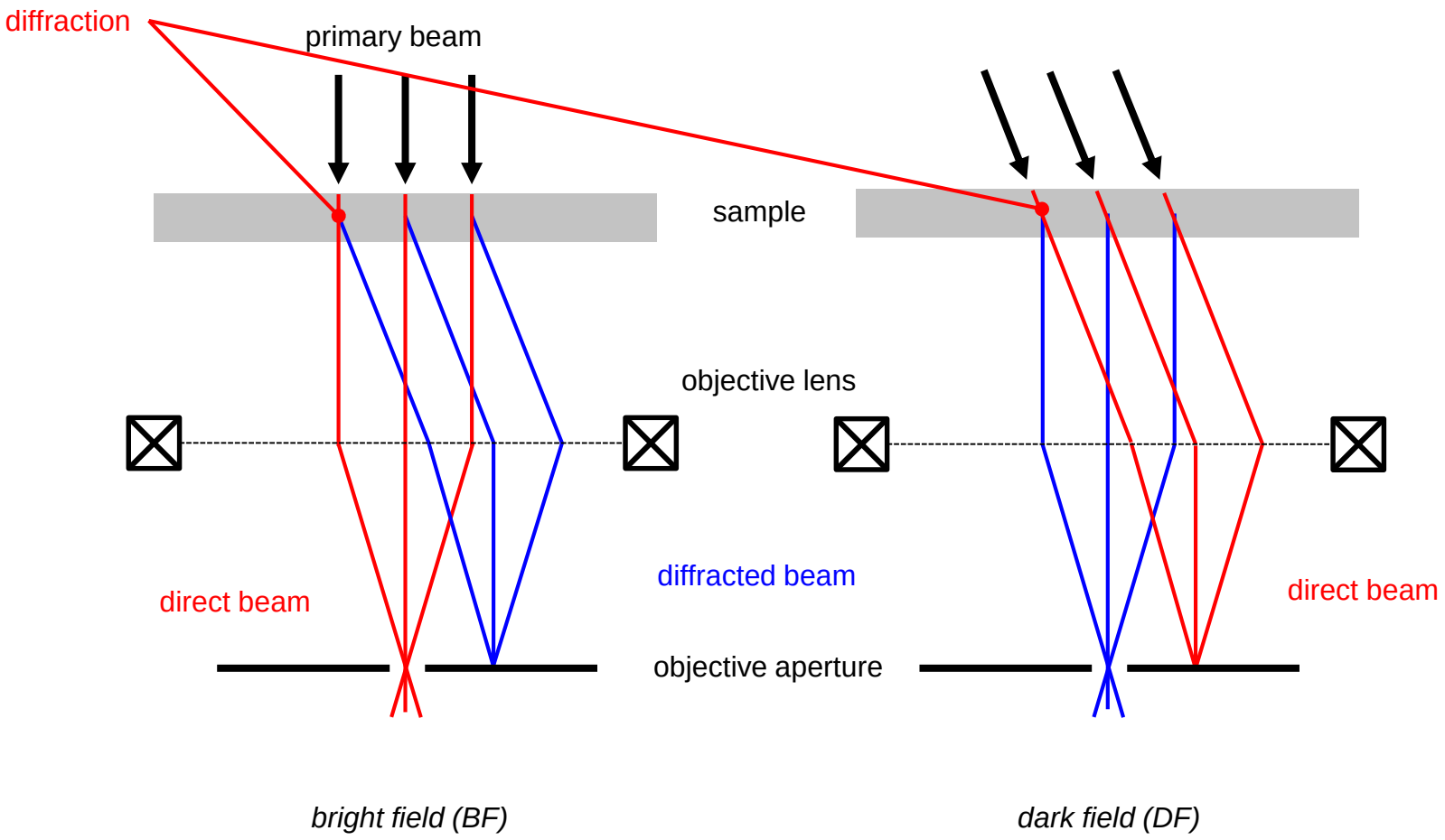

relativistic wave length at 200 kV: $\lambda = 0.0025\ \mathrm{nm}$

Transmission Electron Microscopy (TEM)

Selection of the beam for imaging by proper tilting the beam and positioning of the aperture. For weak beam dark field imaging, higher order spots with larger distance to the primary beam are selected.

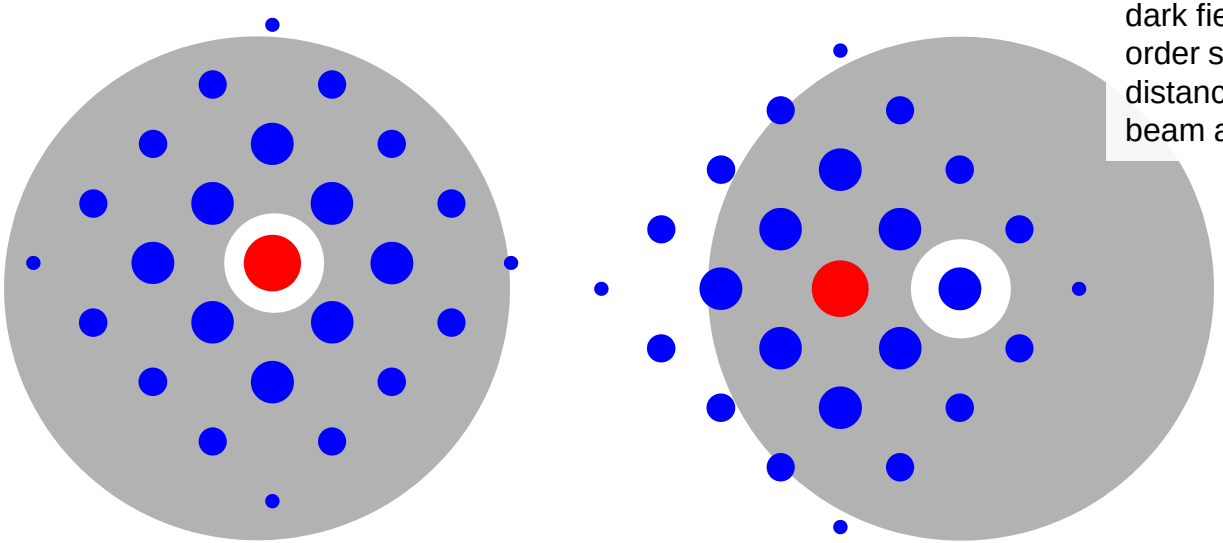

bright field (BF)

dark field (DF)

relativistic wave length at 200 kV: $\lambda = 0.0025$ nm

Transmission Electron Microscopy (TEM)

- The **altered diffraction condition** in the vicinity of the dislocation results in bright or dark field contrast:

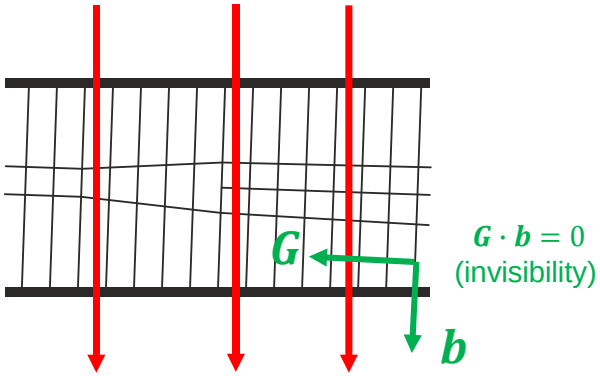

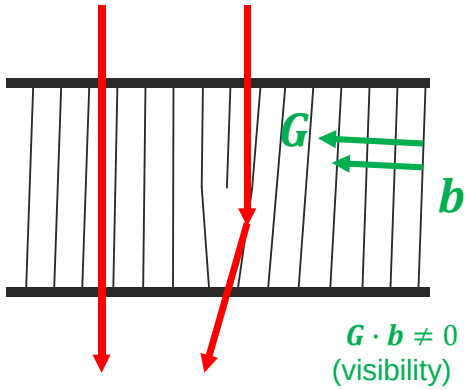

Dislocation are not always visible!

When visible, the **dislocation is dark in BF images**. The position of dislocation is slightly different from the position in the image!

Lateral resolution of BF images is rather **low**.

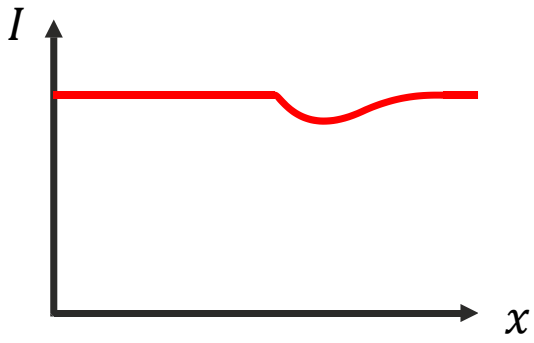

Note that in TEM literature $\boldsymbol{G}$ is typically denoted by a small $\boldsymbol{g}$. For consistency with Ch. 3, we use capital $\boldsymbol{G}$ here because the meaning is the same. Further, the invisibility condition for pure edge dislocations is strictly only achieved when both $\boldsymbol{G} \cdot \boldsymbol{b} = 0$ and $\boldsymbol{G} \cdot \boldsymbol{b} \times \boldsymbol{s} = 0$ are fulfilled due to the strain components perpendicular to the slip plane. This is omitted for the sake of simplicity.

Transmission Electron Microscopy (TEM)

- The **altered diffraction condition** in the vicinity of the dislocation results in bright or dark field contrast:

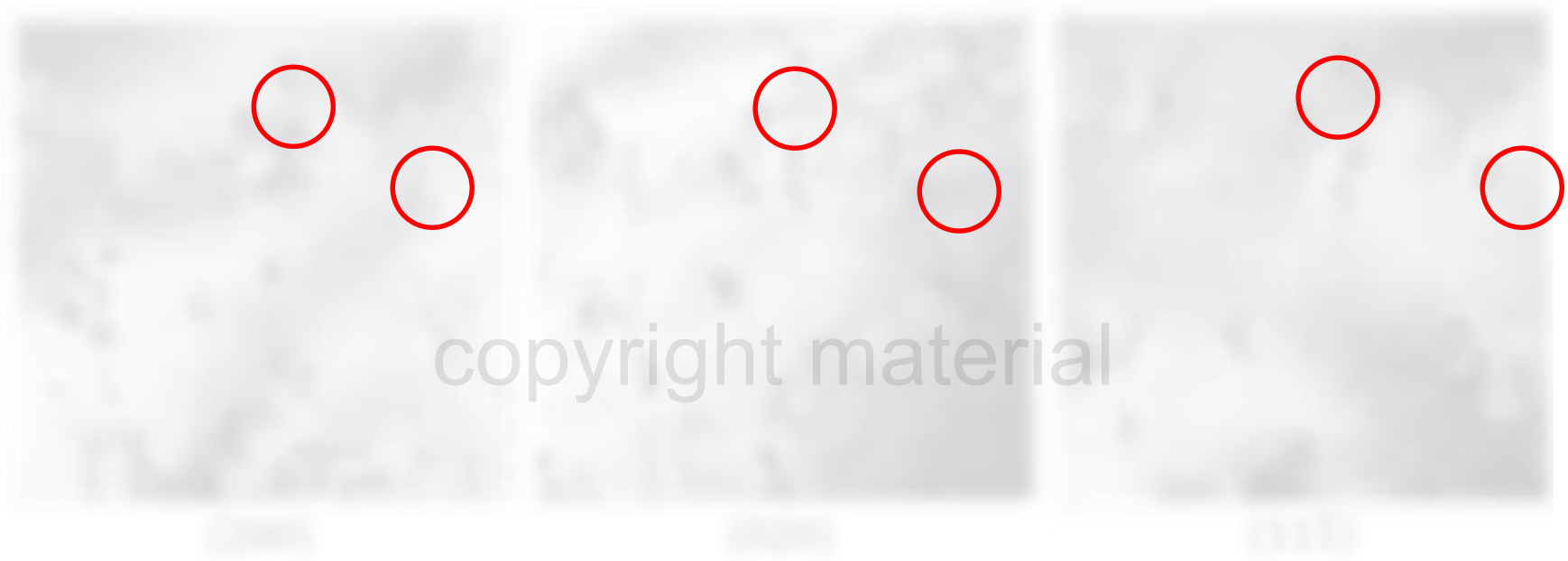

BF images of Al of the same region but with different diffracting planes.

H. Zhang: “Scattering Contrast” (2011), https://www.tcd.ie/Physics/research/groups/pan/teaching/PY5019/notes/Contrast-1.pdf

Transmission Electron Microscopy (TEM)

- When interpreting the images, the **projection of thin foil has to be considered**:

Projection of the dislocation structure in a foil of about 200 nm in thickness.

D. Hull, D. J. Bacon: “Introduction to Dislocations”, Amsterdam, etc.: Elsevier (2011)

Transmission Electron Microscopy (TEM)

- Stacking faults surrounded by partial dislocations are also visible under certain conditions. Depending on inclination and size, a fringe pattern is seen:

D. Hull, D. J. Bacon: “Introduction to Dislocations”, Amsterdam, etc.: Elsevier (2011)

Transmission Electron Microscopy (TEM)

- Stacking faults surrounded by partial dislocations are also visible under certain conditions. Depending on inclination and size, a fringe pattern is seen:

D. Hull, D. J. Bacon: “Introduction to Dislocations”, Amsterdam, etc.: Elsevier (2011)

Transmission Electron Microscopy (TEM)

- Stacking faults surrounded by partial dislocations are also visible under certain conditions. Depending on inclination and size, a fringe pattern is seen:

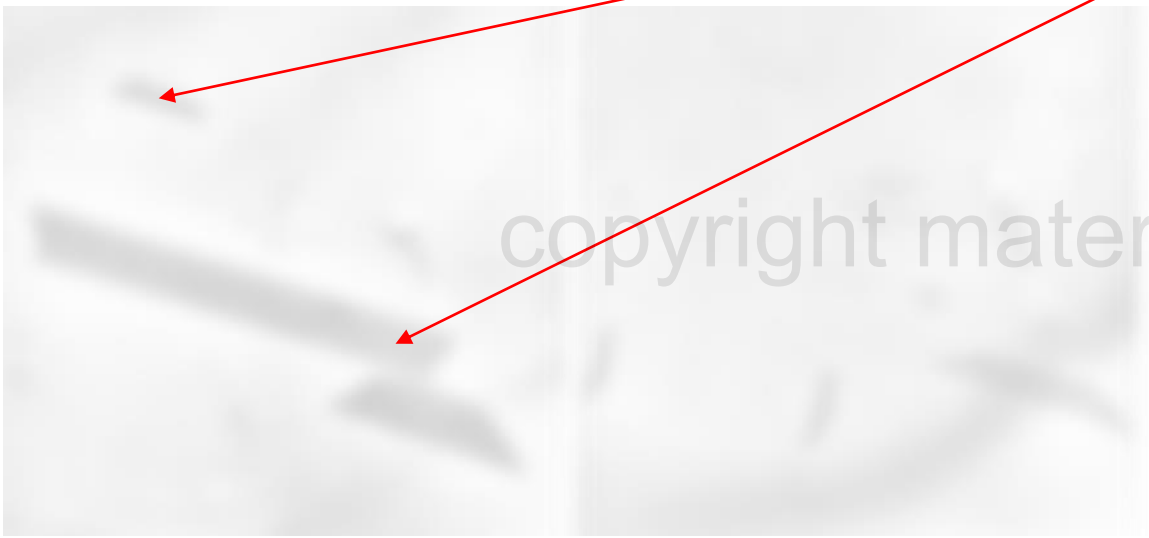

https://www.tf.uni-kiel.de/matwis/amat/def_en/kap_6/advanced/t6_3_2.html

Transmission Electron Microscopy (TEM)

- The **altered diffraction condition** in the vicinity of the dislocation results in bright or dark field contrast:

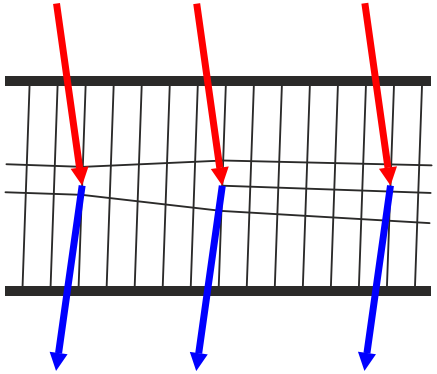

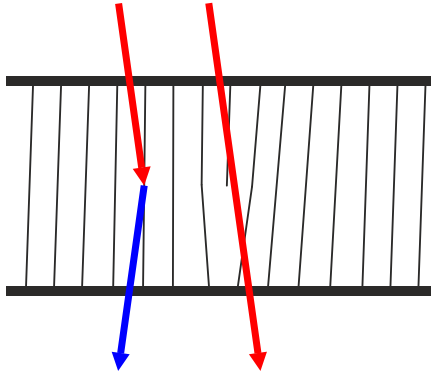

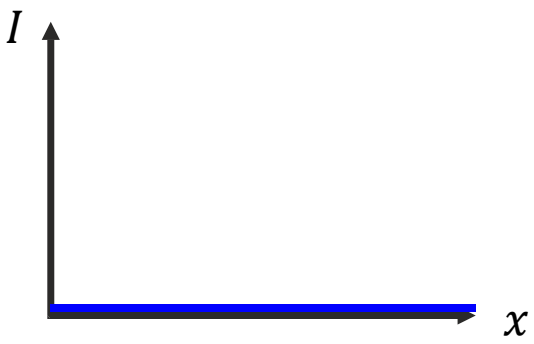

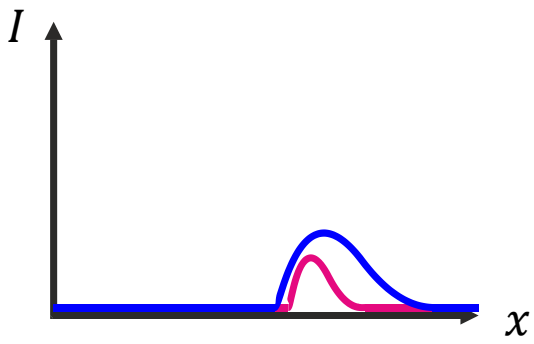

When visible, the **dislocation is bright** in DF mode.

With respect to dislocations, the **lateral resolution of weak beam DF images is higher** then for conventional DF and BF images.

Transmission Electron Microscopy (TEM)

Shockley partial 1

Shockley partial 2

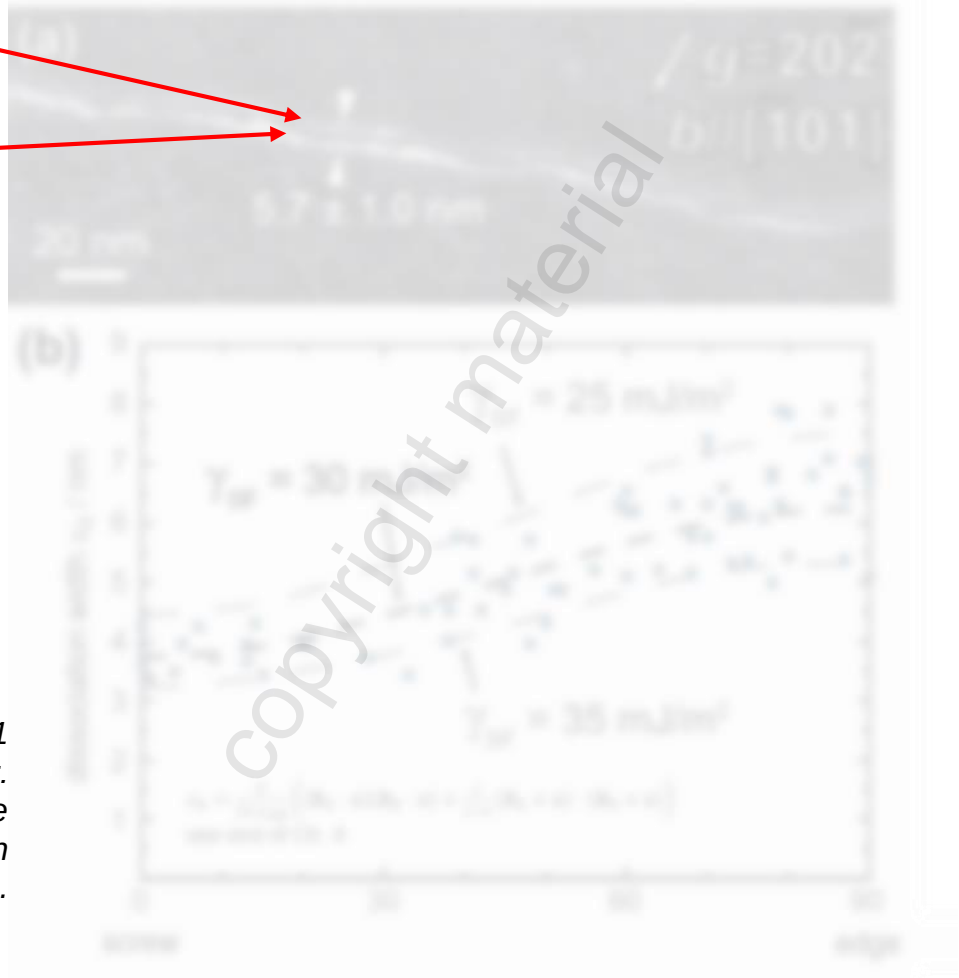

Dissociated dislocation in CoCrFeMnNi (A1 alloy) in DF „weak-beam“ contrast. The dissociation width depends on the character of the un-dissociated dislocation and the intrinsic stacking fault energy γ_{SF}.

N. Okamoto et al.: “Size effect, critical resolved shear stress, stacking fault energy, and solid solution strengthening in the CrMnFeCoNi high-entropy alloy”, Scientific Reports 6 (2016) 35863

Transmission Electron Microscopy (TEM)

Note the slight blur at the dislocation lines as a result of relaxation of the lattice at the termination of the dislocation line at the surfaces of the TEM lamella by twisting.

Direct imaging of atomic columns at partial edge dislocation in $SrTiO_3$

W. Sigle et al.: “Dislocations in plastically deformed $SrTiO_3$”, Philosophical Magazine 86 (2006) 4809-4821

Transmission Electron Microscopy (TEM)

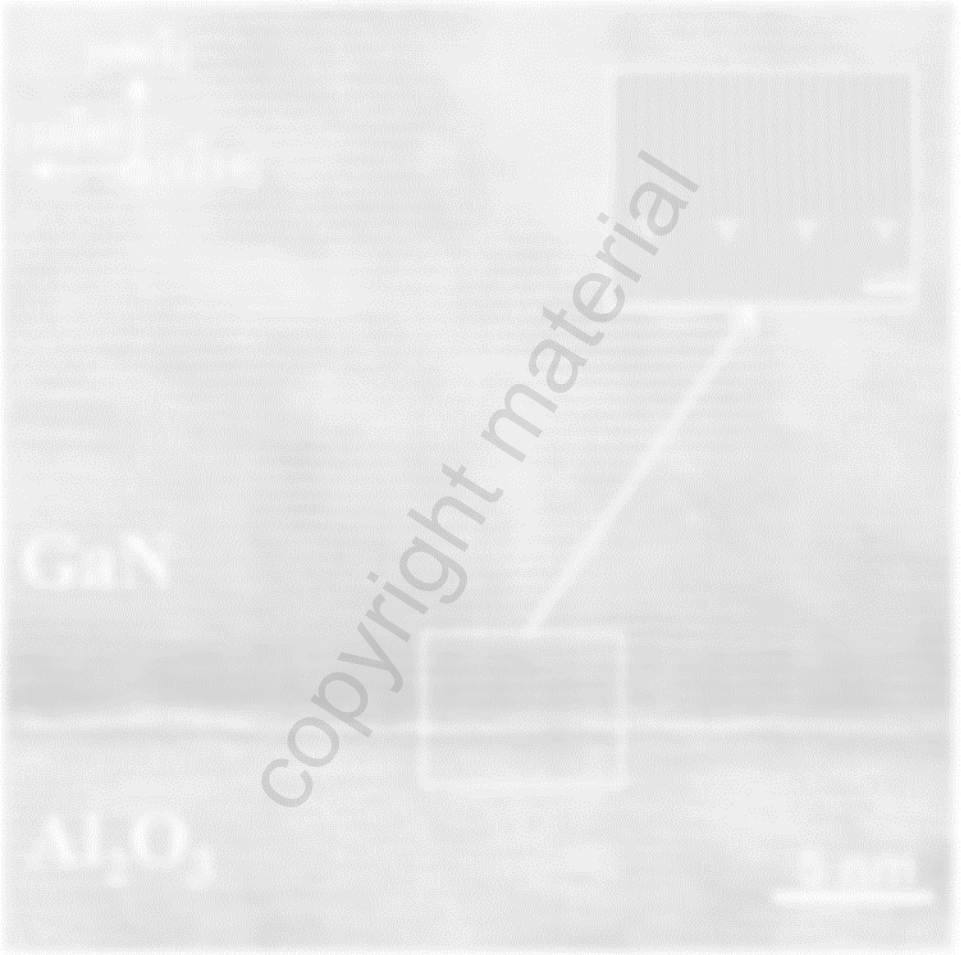

Direct imaging of atomic columns at an nitride/oxide-interface with misfit dislocations. FFT filtering of $(10\bar{1}0)_{GaN}$ *and* $(1\bar{1}\bar{1}0)_{Al_2O_3}$ *reveals the edge dislocations.*

T. D. Young et al.: “3D modelling of misfit networks in the interface region of heterostructures”, J. Phys. D: Appl. Phys. 40 (2007) 4084-4091

Transmission Electron Microscopy (TEM)

- **Dislocations can be observed by TEM**.
- Dislocations are **only visible under certain conditions**. The **systematic investigation of visibility and invisibility** allows for the **determination of the Burgers vector** ($\boldsymbol{g} \cdot \boldsymbol{b} = 0$).
- The **determination of dislocation density is difficult** due to: **uncertain volume** (can be estimated under certain conditions), **projection of the dislocation structure** and the **visibility/invisibility of dislocations**.
- Atomic resolution in HR-TEM can be used to image the **atomic columns at dislocations**; apart from some very special evaluations, only edge components are imaged.
- **Improved lateral resolution** is achieved by utilizing **“weak beam”-DF** imaging.

Scanning Electron Microscopy (SEM)

- In the scanning electron microscope, a **bulk sample is illuminated and scanned with an electron beam** and the **interaction products are detected** point-wise.
- A large **variety of interaction products** is observed.
- The **lateral resolution** of each imaging mode strongly **depends on the type and energy of the interaction products**. Therefore, in most cases a **correlation with the acceleration voltage** is observed.

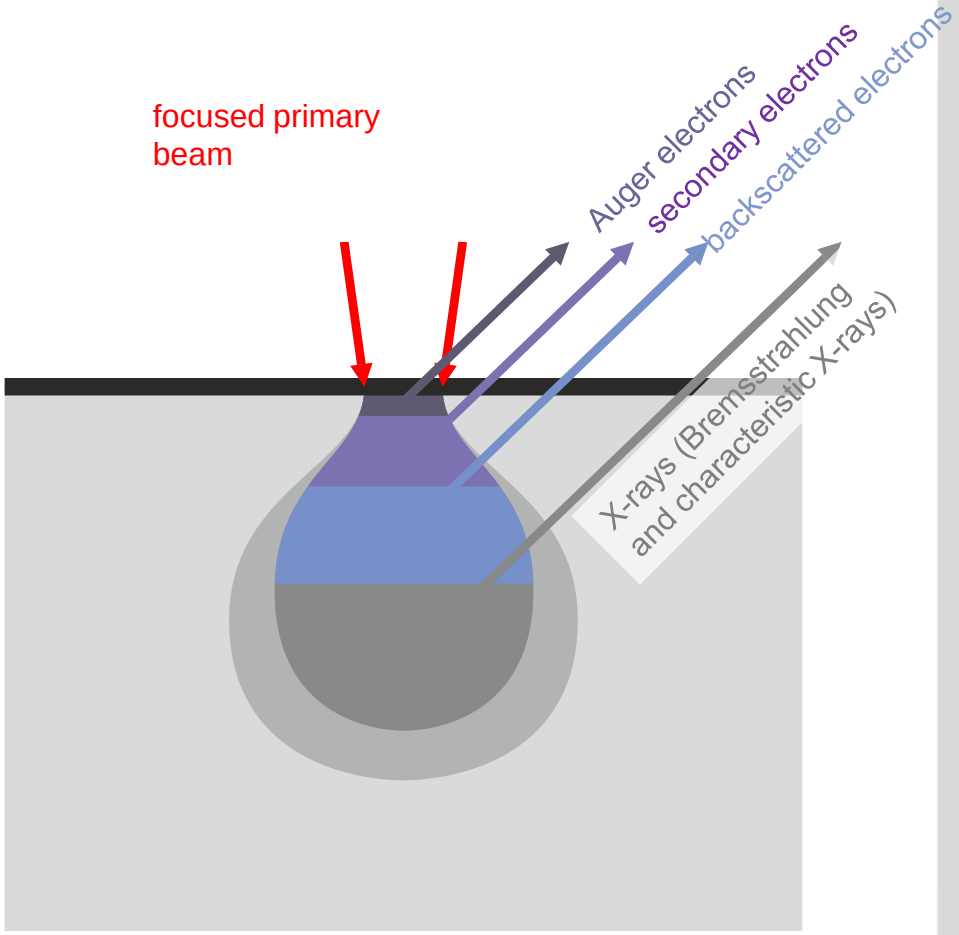

Electron Channeling Contrast Imaging (ECCI)

- Some of the primary electrons are (quasi-)elastically scattered by the solid. Most of the scattering is in the direction of the primary beam (no tilt of the sample). These electrons are called **backscattered electrons** (BSE).
- BSE have rather **small Bragg angles** according to their wavelength (at almost the entire energy corresponding to the acceleration voltage) and the typical lattice plane spacing in metallic materials. Under certain conditions (slightly inclined crystal), the **electrons deeply penetrate the crystal by iterative diffraction** at the lattice planes **(„channeling“)**. After a scattering event, the electrons cannot leave the solid anymore due to large penetration. **The intensity of BSE is thus reduced under such conditions**.
- Since the Bragg angle is rather small, **imaging of crystal defects with long-range displacement/distortion fields** is possible.
- The imaging requests an almost **defect-free metallographic surface preparation**.
- The above-described contrast formation is much simplified. The details are similar to channeling in the TEM and quantitative requires much more physical modeling of the electron waves and the solid.

Electron Channeling Contrast Imaging (ECCI)

Compare the contrast resulting from the displacement field to the elastic solution later in Ch. 4c.

Screw dislocations with dislocation line perpendicular to the sample surface in GaN for different diffraction conditions. Note the contrast change.

R. J. Kamaladasa & Y. N. Picard: “Basic Principles and Application of Electron Channeling in a Scanning Electron Microscope for Dislocation Analysis” in “Microscopy: Science, Technology, Applications and Education” by A. Méndez-Vilas and J. Díaz (Eds.) Badajoz: Formatex Research Center (2010)

Electron Channeling Contrast Imaging (ECCI)

Recrystallized regions with low defect density, few dislocations and no oxide dispersoids.

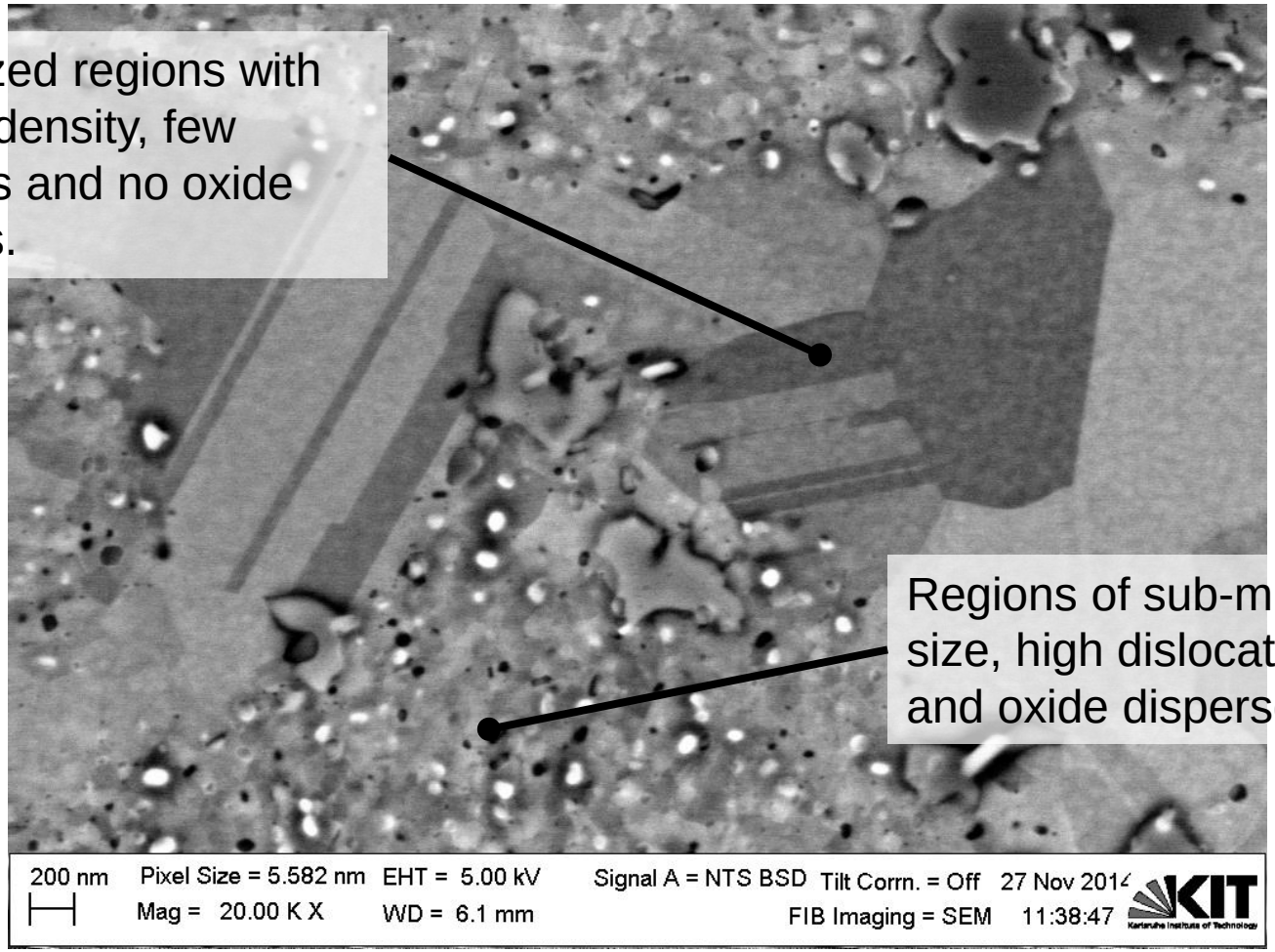

Imaging of a mechanically alloyed and consolidated austenitic ODS steel.

Electron Channeling Contrast Imaging (ECCI)

Welsch, M.: “Anwendungen des Electron Channeling Contrast Imaging (ECCI)”, Mitarbeiterseminar des WWM der Universität des Saarlandes (2004)

Electron Channeling Contrast Imaging (ECCI)

- **ECCI provides similar imaging of dislocation as in the TEM** but significantly **larger fields of view** can be achieved.
- In conjunction with electron backscatter diffraction (EBSD), controlled diffraction conditions can be achieved and a determination of the Burgers vector of the dislocations becomes possible. In most cases, channeling condition is achieved by accident; the method is then sometimes called pseudo-ECCI.

Field Ion Microscopy (FIM)

- In the FIM, high tension is applied to a small, very sharp tip at temperatures of 20 to 100 K in a low pressure noble gas atmosphere. The atoms of the noble gas can be ionized due to the high electrical fields (edge effect) at tip under certain conditions which prevent field evaporation of the sample atoms. The ions are accelerated by the high tension and imaged on screen.
- The image represents a projections of the surface structure.

Field Ion Microscopy (FIM)

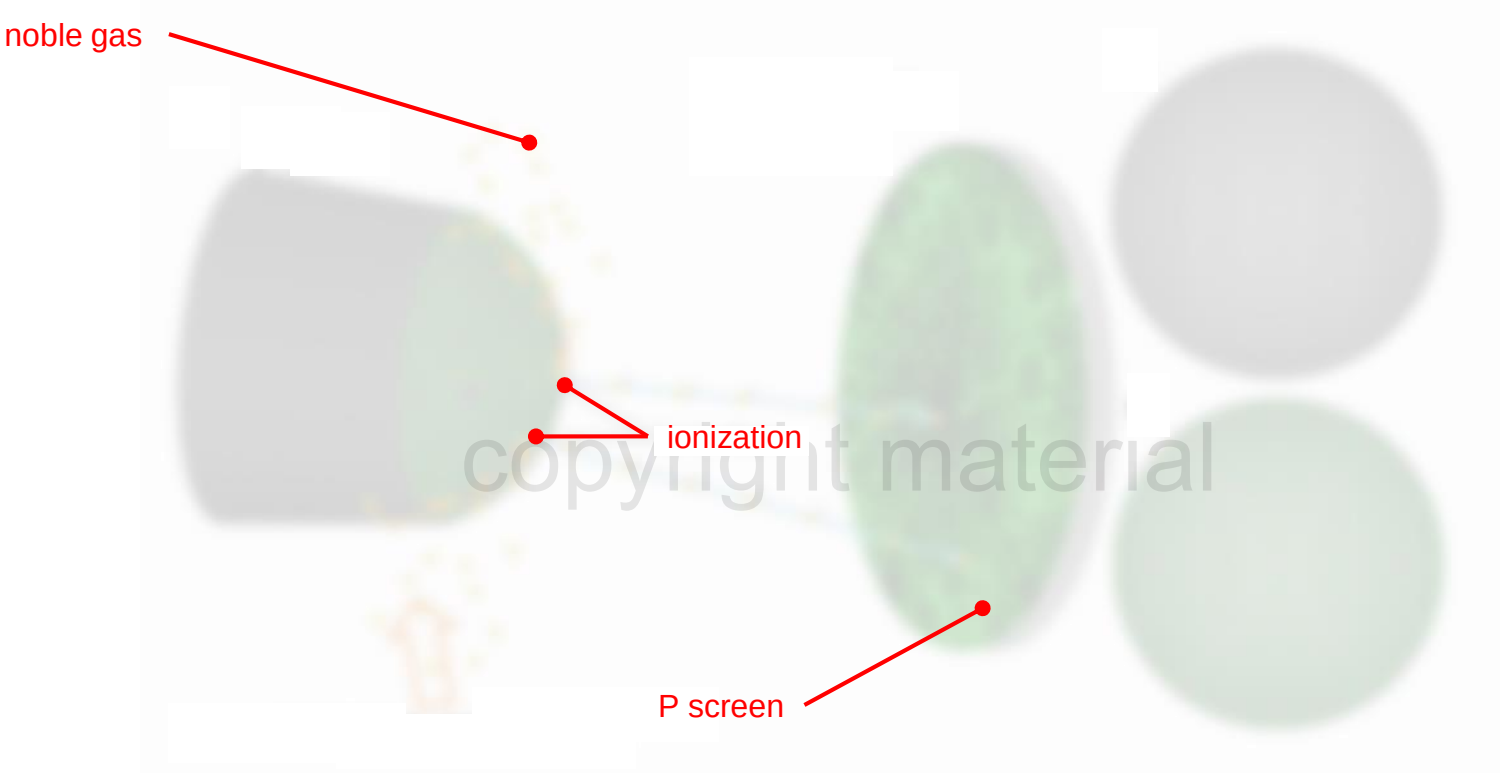

Scheme of FIM.

B. Gault et al.: “Atom Probe Microscopy”, Springer Series in Materials Science 160, New York, USA: Springer (2012)

Field Ion Microscopy (FIM)

Imaging of an Fe tip containing a dislocation.

B. Gault et al.: “Atom Probe Microscopy”, Springer Series in Materials Science 160, New York, USA: Springer (2012)

Electron Backscatter Diffraction (EBSD)

- The same BSE as for ECCI can also be used in analytical SEM.
- In order to increase BSE yield, the sample tilted with respect to the primary beam (electrons become scattered in forward direction, FSE). There is a **characteristic pattern formed by diffraction of scattered electrons**, which can be imaged on a P screen.
- The **orientation of Kikuchi lines and its comparison to the sample coordinate system** allows the **identification of the crystal structure** and of the **orientation of the crystal portion in the probe volume**.

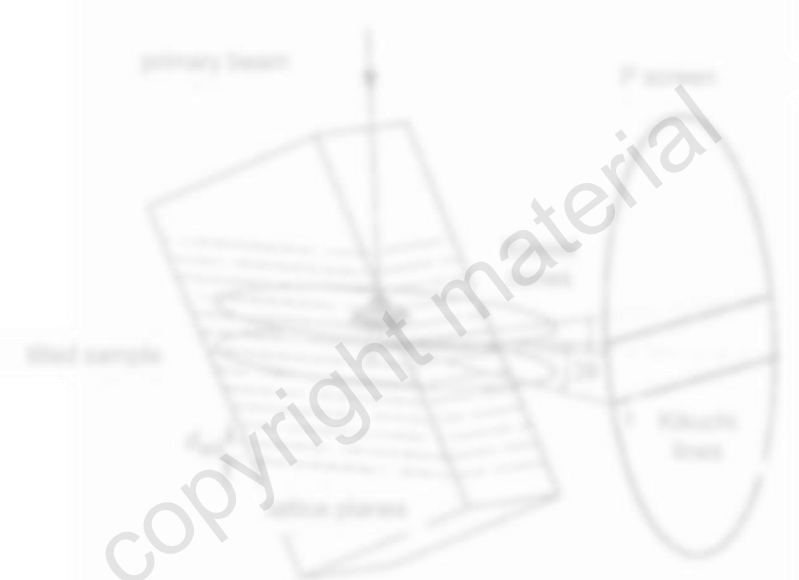

http://www.mineralsocal.org/micro/images/ebsdfig1.gif

Electron Backscatter Diffraction (EBSD)

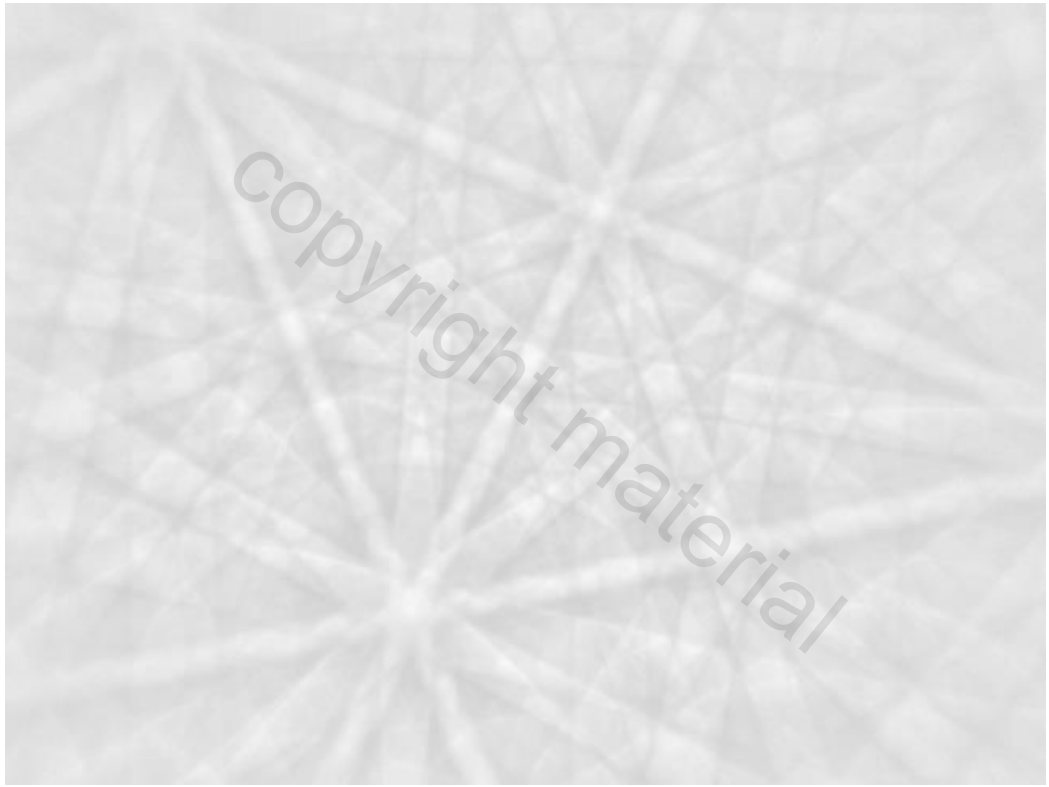

Kikuchi pattern of Ni.

http://www.ebsd.com/ebsd-applications/ebsd-gallery/diffraction-patterns-from-various-materials

Electron Backscatter Diffraction (EBSD)

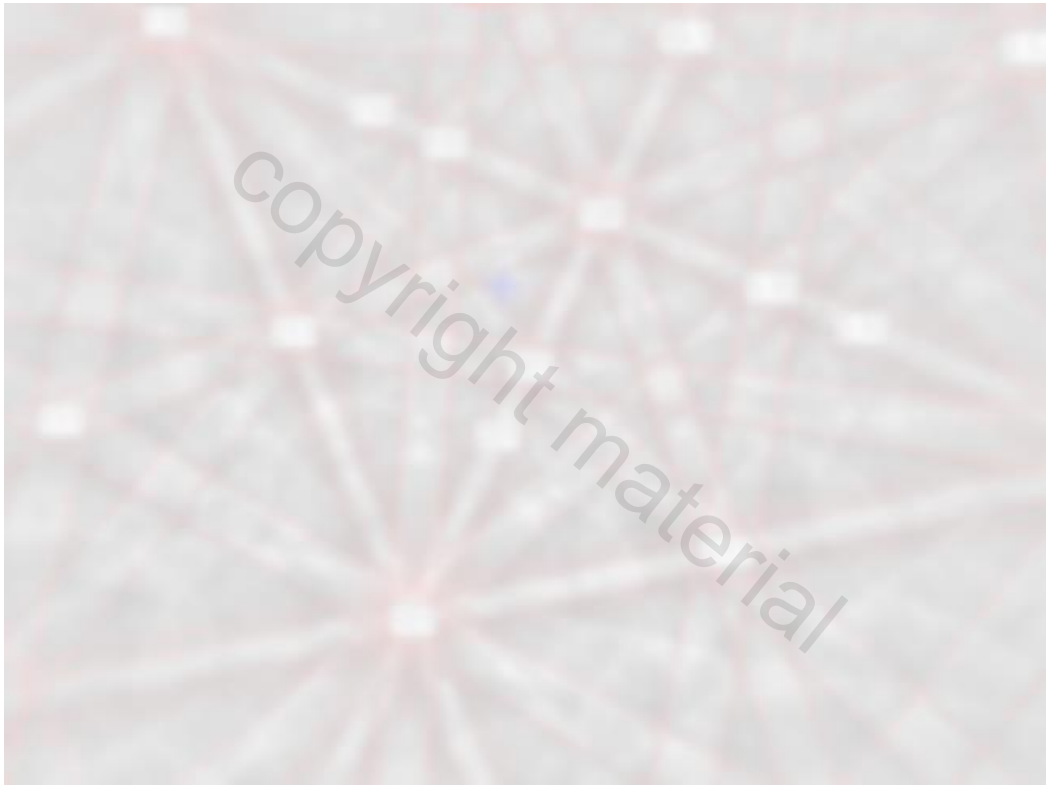

Indexed Kikuchi pattern of Ni (A2, Cu structure type) with band edges.

http://www.ebsd.com/ebsd-applications/ebsd-gallery/diffraction-patterns-from-various-materials

Electron Backscatter Diffraction (EBSD)

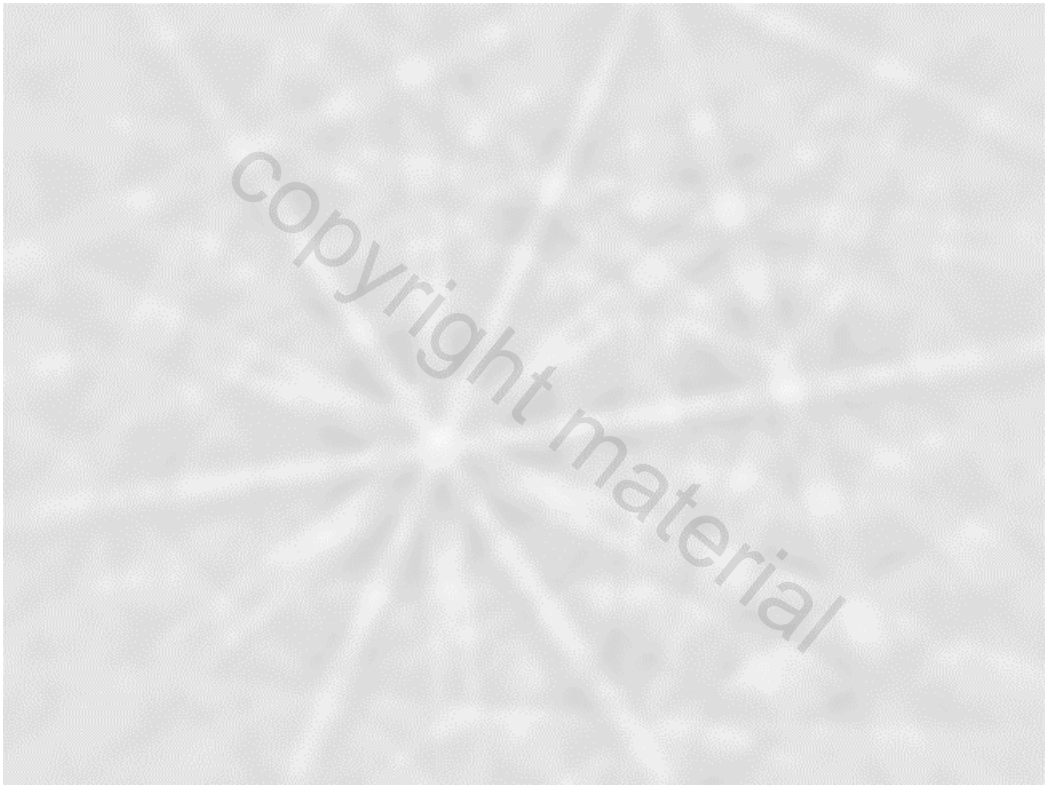

Kikuchi pattern of α-Fe.

http://www.ebsd.com/ebsd-applications/ebsd-gallery/diffraction-patterns-from-various-materials

Electron Backscatter Diffraction (EBSD)

Since the extension rules are different to the Cu structure type, the reflecting plane sets and zone axes are different. Compare to the slide before.

Indexed Kikuchi pattern of α-Fe (A1, W structure type) with band edges.

http://www.ebsd.com/ebsd-applications/ebsd-gallery/diffraction-patterns-from-various-materials

Electron Backscatter Diffraction (EBSD)

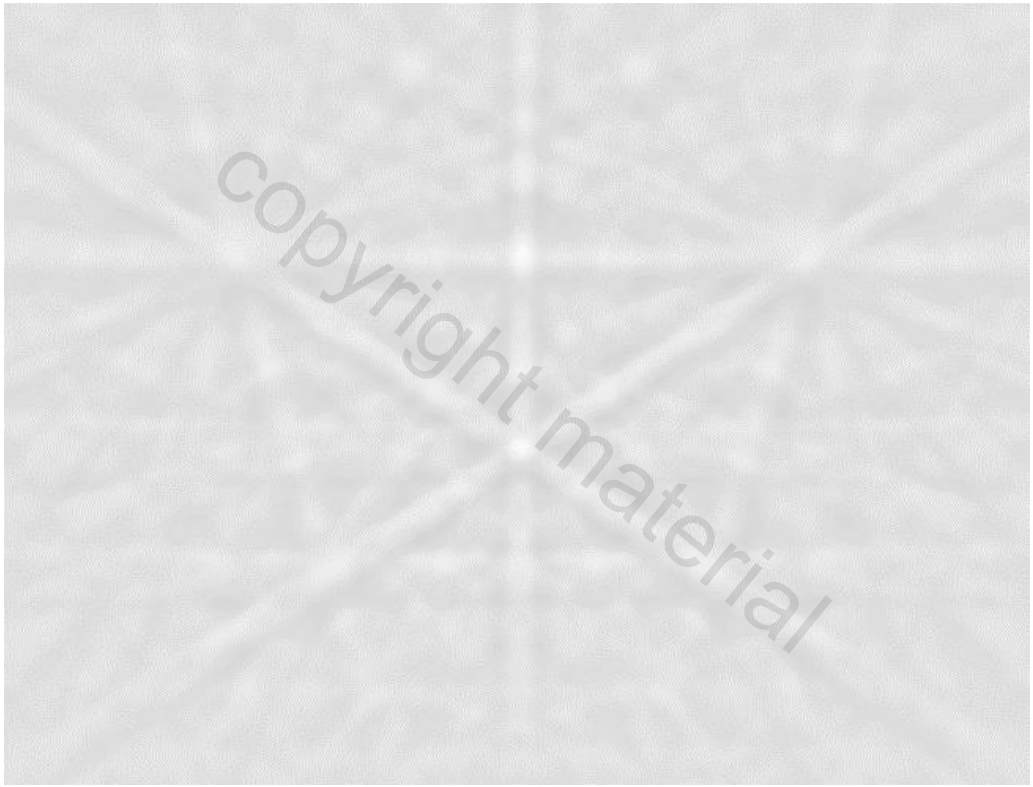

Kikuchi pattern of Si; same Bravais type of lattice and similar symmetry as Ni but due to two atomic basis much more multi-bands.

http://www.ebsd.com/ebsd-applications/ebsd-gallery/diffraction-patterns-from-various-materials

Electron Backscatter Diffraction (EBSD)

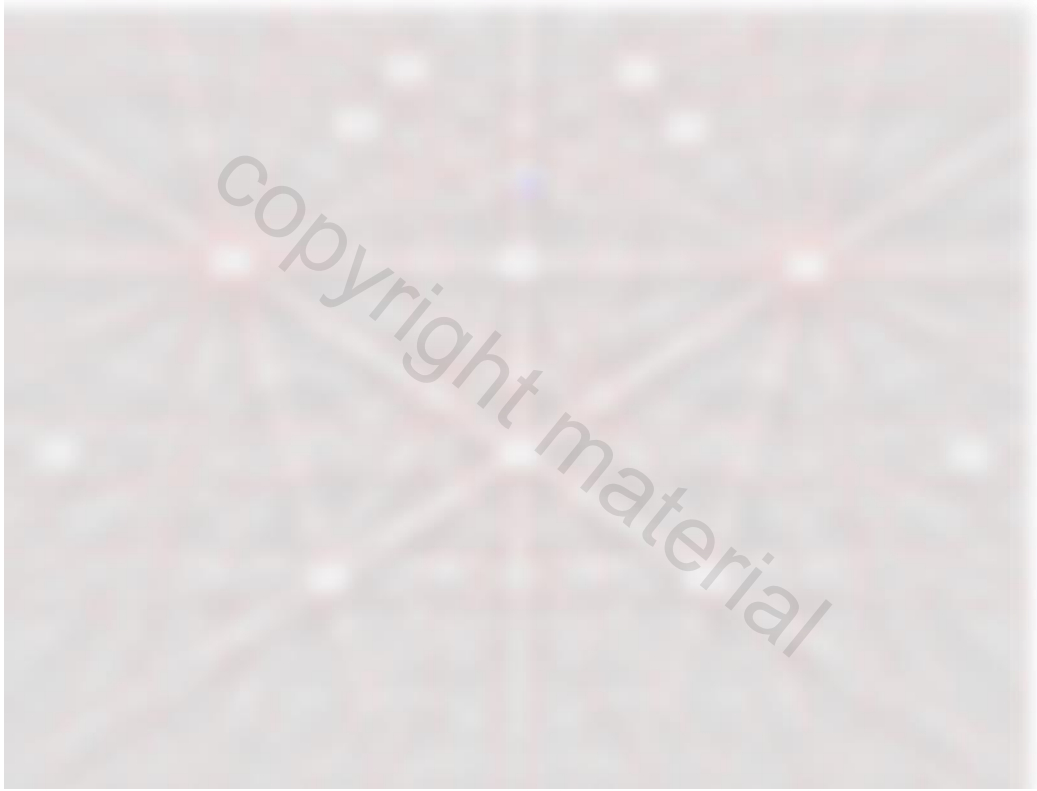

Indexed Kikuchi pattern of Si (A4, diamond structure type) with some band edges.

http://www.ebsd.com/ebsd-applications/ebsd-gallery/diffraction-patterns-from-various-materials

Electron Backscatter Diffraction (EBSD)

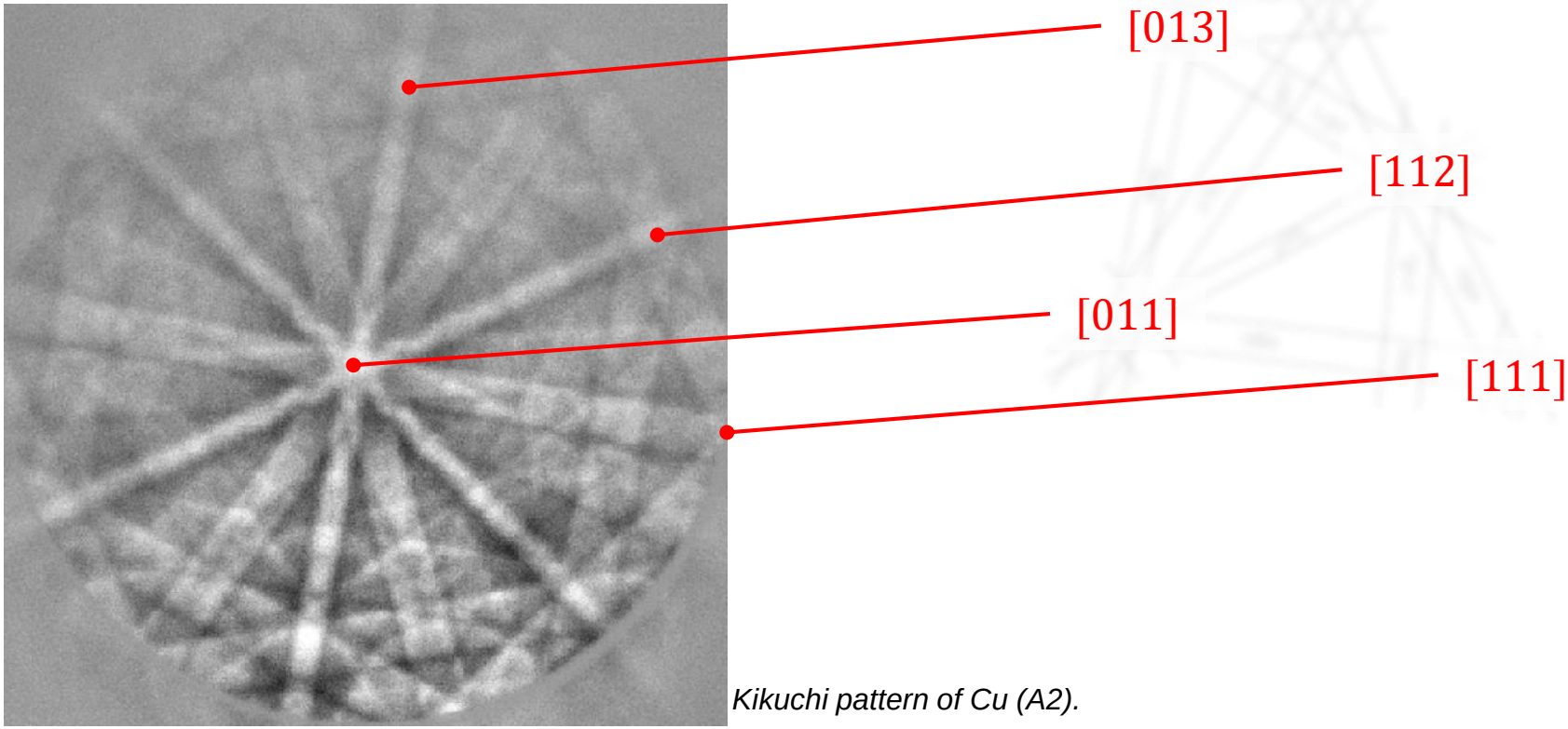

Kikuchi pattern of Cu (A2).

Electron Backscatter Diffraction (EBSD)

- The patterns contain information about dislocations.
- **Statistically stored dislocations reduce the quality of the pattern**, which is quantified during the scans (intensity of the bands in Hough space).
- By using image quality, recrystallized and deformed regions in microstructures can be distinguished.
- Quantification of image quality is difficult due to secondary influences like surface topography.

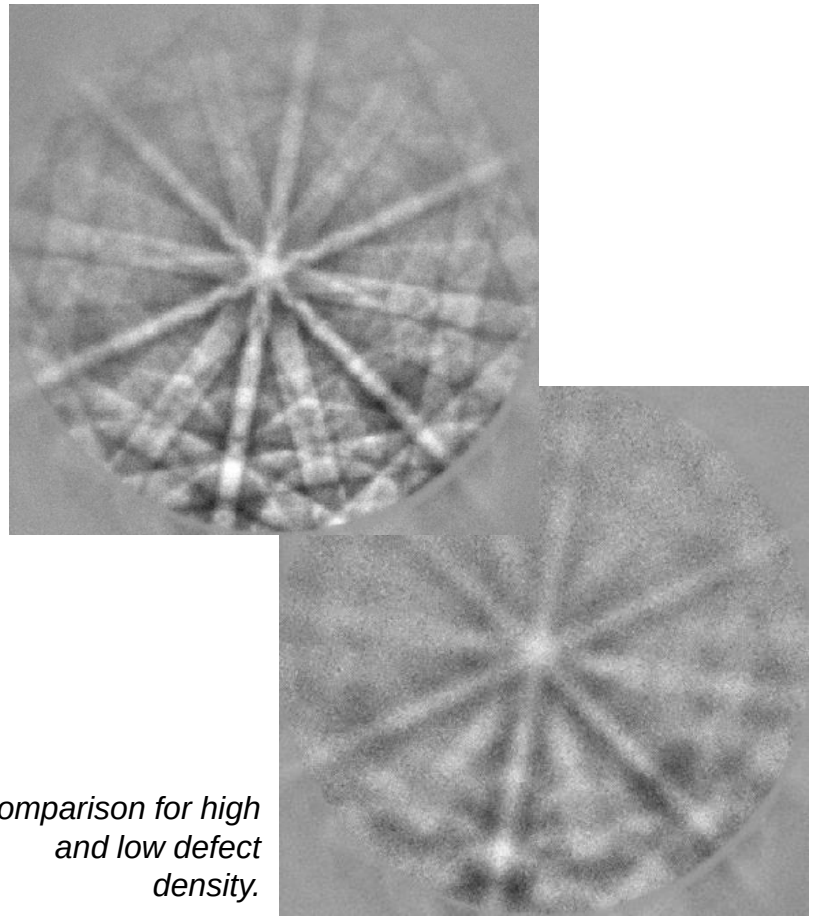

Comparison for high and low defect density.

Electron Backscatter Diffraction (EBSD)

Significantly higher image quality in the recrystallization nucleus.

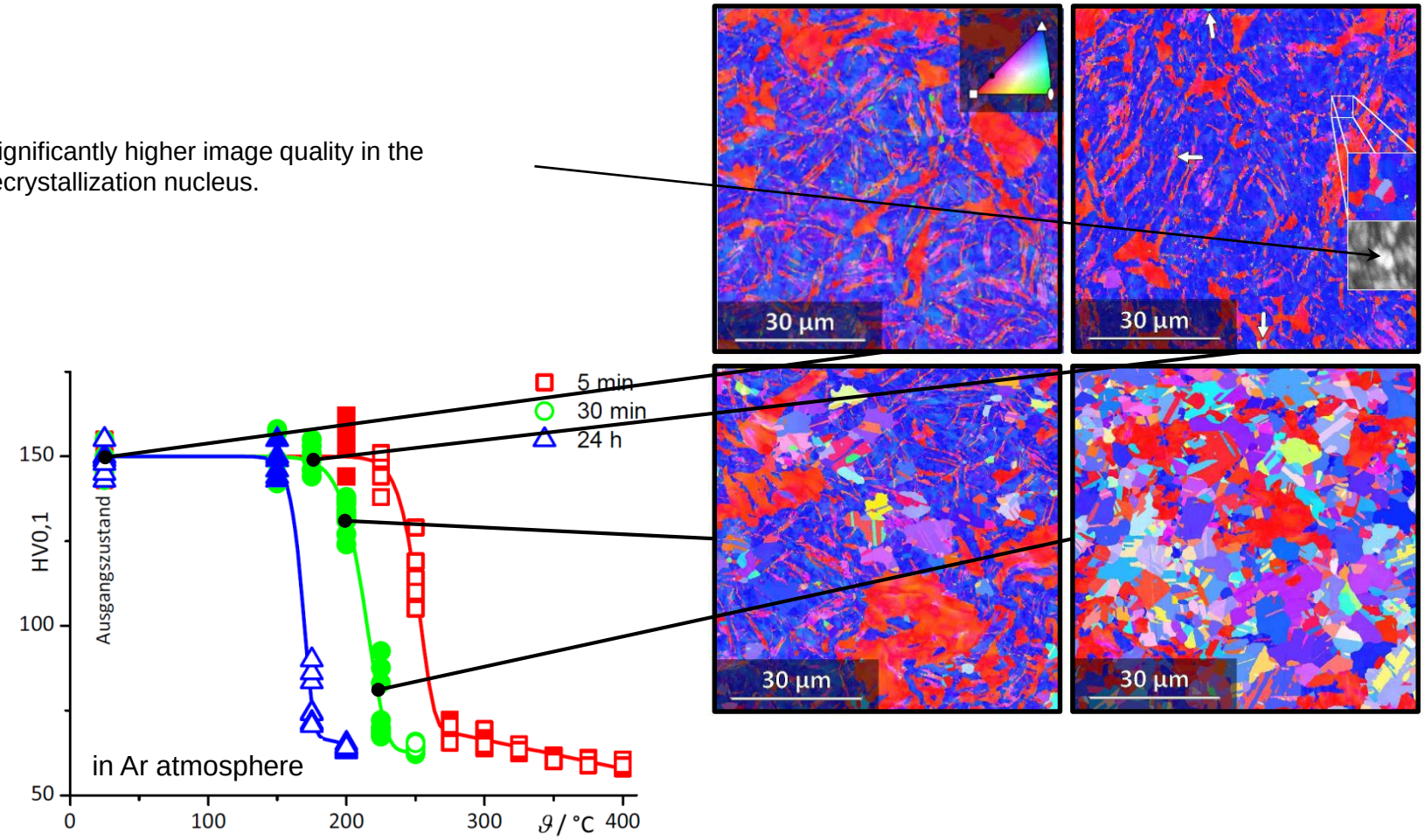

A. Kauffmann, D. Geissler, J. Freudenberger:
"Thermal stability of electrical and mechanical properties of cryo-drawn Cu and CuZr wires", Mat. Sci. Eng. A 651 (2016) 567-573

Electron Backscatter Diffraction (EBSD)

- **Geometrically necessary dislocations (GND) cause small lattice rotations within crystals.**
- The small orientation changes can be detected using EBSD. By utilizing proper models for dislocation arrangements, the density of GND can be re-calculated.

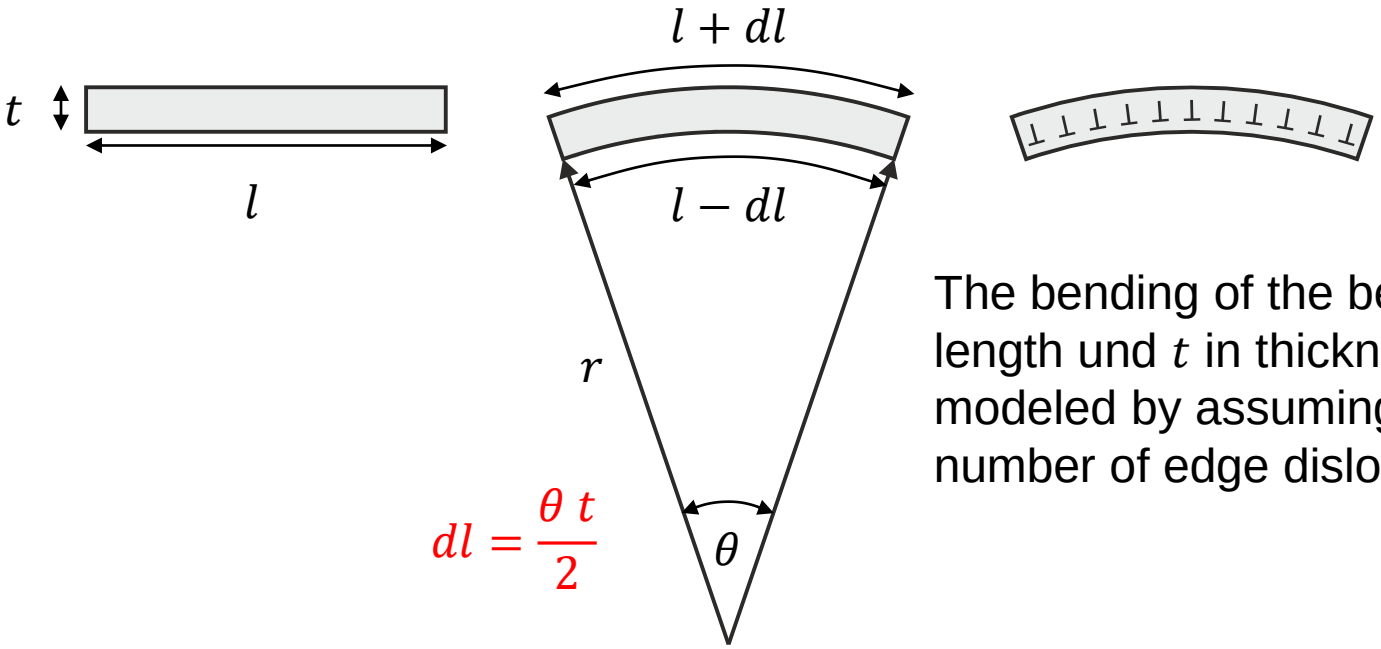

The bending of the beam of l in length und t in thickness can be modeled by assuming a certain number of edge dislocations.

Electron Backscatter Diffraction (EBSD)

- The number of lattice planes at the outer fiber under tension is $^{l+dl}/_{b}$ when the lattice plane spacing corresponds to the Burgers vector. At the opposite, $^{l-dl}/_{b}$ lattice planes are needed.
- The density of edge dislocations is hence:

$$\rho \approx \frac{{}^{l+dl}/_{b} - {}^{l-dl}/_{b}}{l\,t} = \frac{2\,dl}{l\,t\,b} = \frac{\theta}{l\,b}$$

- The point-to-point misorientation is θ and the step size is l.
- The result significantly depends on the validity of the assumed model of the dislocation arrangement!

Electron Backscatter Diffraction (EBSD)

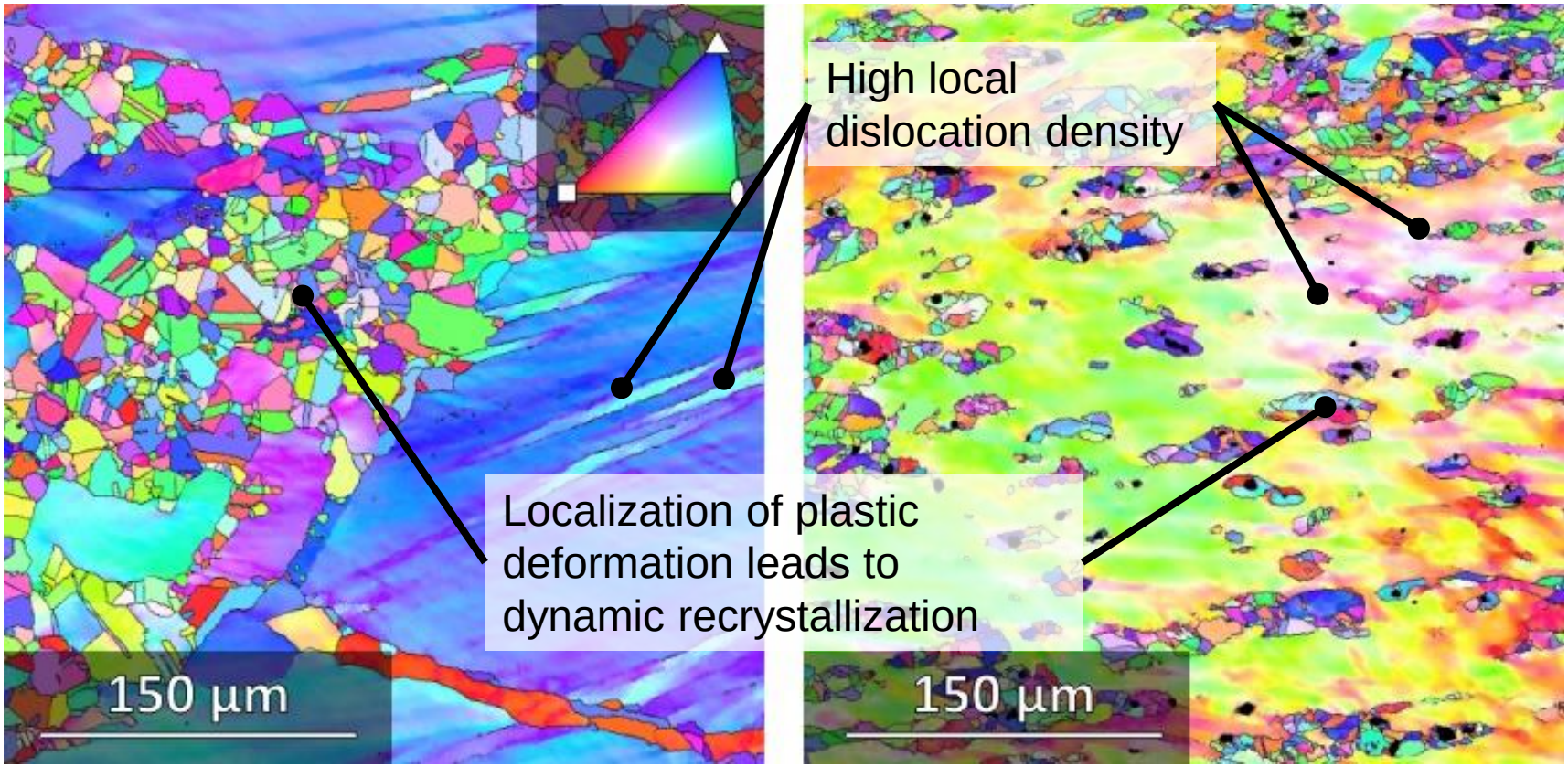

High local misorientations during hot-working of CuAgZr alloys: (left) no secondary phase; localization at grain boundaries, (right) secondary phase particles (5 to 10 µm, black regions) lead to localization within the grains.

A. Kauffmann, IFW Dresden (2012)

Cross-Correlation HR-EBSD

- An **increased angular resolution** is achieved by **comparing different regions in the Kikuchi patterns against standard patterns** by utilizing **cross-correlation**.
- Apart from the orientation information, **information about the changes of the zone axes within the probe volume** becomes available.
- Not only point-to-point misorientation is then used for strain analyses, but also the distortion of the unit cells within the probe volume.
- Evaluation is in most cases based on models by Nye and Kröner which consider gradients in rigid body rotation and strain in relation to geometrically necessary dislocation densities.

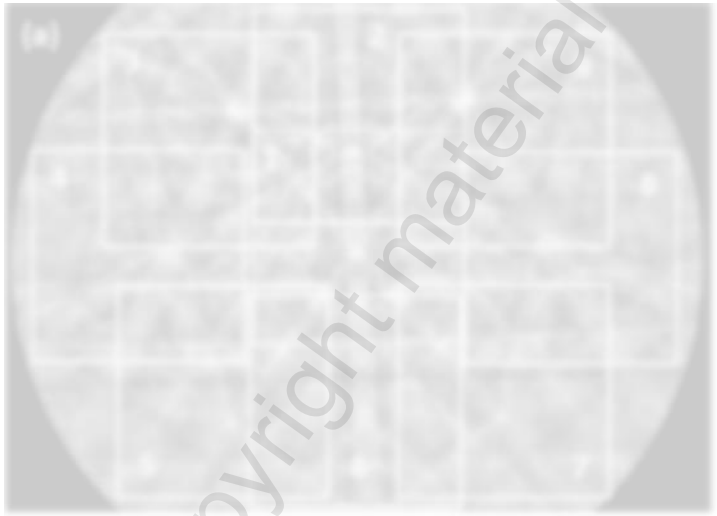

See further details here:

J. Nye: “Some geometrical relations in dislocated crystals”, Acta Metallurgica 1 (1953) 153-162
E. Kröner: “Kontinuumstheorie der Versetzungen und Eigenspannungen”, Ergebnisse der Angew. Mathematik 5 (1958) 1-180
A.Vilalta-Clemente et al.: “Cross-correlation based high resolution electron backscatter diffraction and electron channelling contrast imaging for strain mapping and dislocation distributions in InAlN thin films”, Acta Materialia 125 (2017) 125-135

Electron Backscatter Diffraction (EBSD)

- Electron backscatter diffraction provides **different types of information about dislocation density**:
  - **Qualitative**: Pattern quality contains information about statistically stored dislocations within the probe volume. Gradients of crystal orientation mapped by point-to-point misorientations are indicative of geometrically necessary dislocations.
  - **Quantitative**: By utilizing proper models of the dislocation structures, the density of geometrically necessary dislocations can be calculated.

Etch Pits

- **Dislocation lines terminating at polished surfaces can be etched**. The etch pits exhibit distinct crystallographic planes depending on the type of the dislocation.
- When dislocation density is not too high, dislocation density can be estimated by counting the etch pits per surface area.

D. Hull, D. J. Bacon: “Introduction to Dislocations”, Amsterdam, etc.: Elsevier (2011)

Etch Pits

D. Hull, D. J. Bacon: “Introduction to Dislocations”, Amsterdam, etc.: Elsevier (2011)

Etch Pits

Etch pits on recrystallized, coarse grained Cu. Due to different orientation of the etch pits in different grains, contrast by micro-roughness is observed at low magnification.

A. Kauffmann, IFW Dresden (2012)

significant micro roughness due to etch pits.

etch pits in grains of different orientations

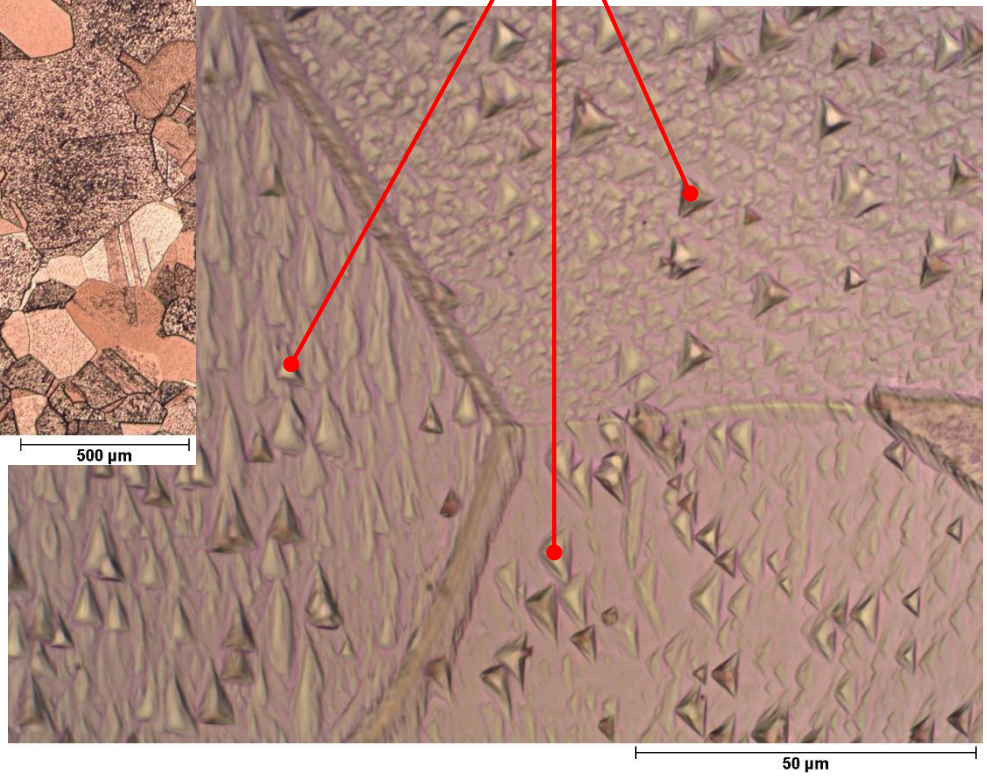

Etch Pits

Etch pits at a LAGB in Ge. The LAGB is formed from a metastable arrangement of stacked dislocations with distances of several microns.

D. Hull, D. J. Bacon: “Introduction to Dislocations”, Amsterdam, etc.: Elsevier (2011)
Vogel et al.: “Observation of Dislocation in Lineage Boundaries in Germanium”, Physical Review 90 (1953) 489

Electrical Resistivity

- Ideal crystals of metallic materials (no defects, infinite volume, no thermal fluctuations, 0 K ground state) have no resistivity.
- Two types of changes by defects are observed:
  - At elevated temperatures, a linear temperature dependence of the electrical resistivity is observed $\rho \approx \rho_0 + \rho_0\, \alpha\, \Delta T$ with a dominating phonon scattering contribution. According to Matthiesen rule $\rho_0\, \alpha\ \approx \mathrm{const.}$ when defects are introduced. ρ_0 is thereby increasing due to scattering at the defects.
  - At low temperatures, $\rho \propto\ T^5$ is found. The residual resistivity at 0 K is a precise quantity for all kinds of defects.

A. Matthiessen, C. Vogt:
“Ueber den Einfluss der Temperatur auf die elektrische Leitungsfähigkeit der Legirungen“ Pogg. Annalen der Physik 198 (1864) 19-78

Electrical Resistivity

- Base resistivity of Cu-Zn increases with increasing Zn content due to additional Zn atoms acting as scattering centers. Matthiesen rule with $\rho_0 \, \alpha \approx \text{const.}$ is nicely met.
- During recrystallization stored dislocations and deformation twins are removed as scattering centers.

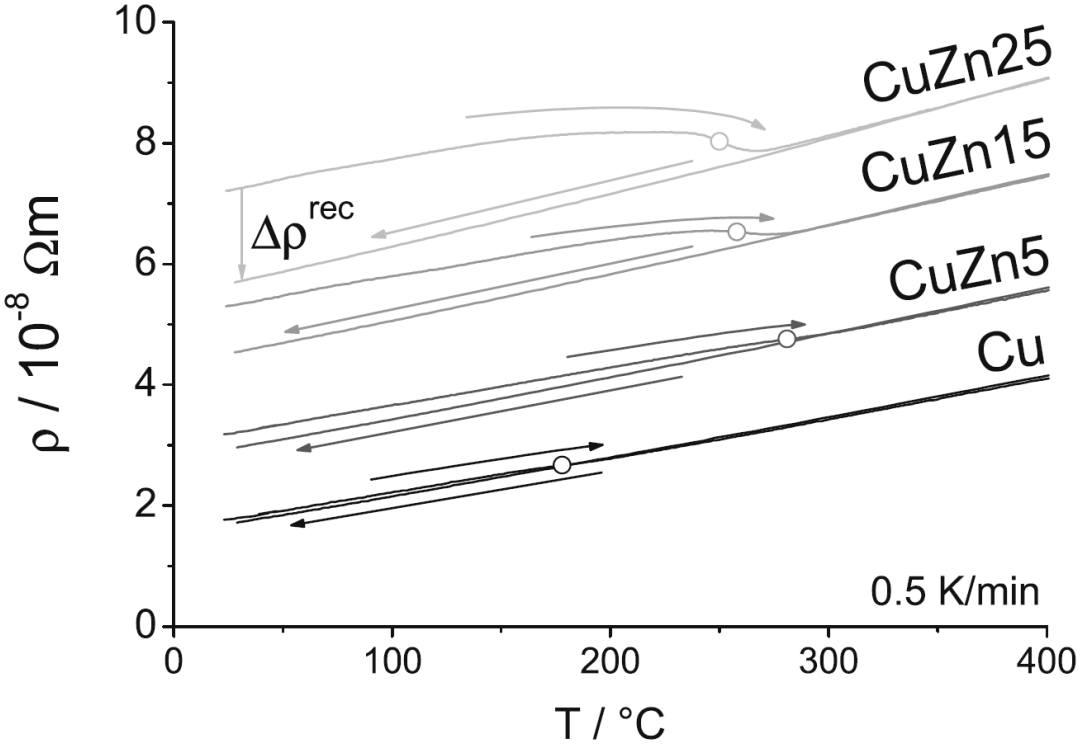

Resistivity of CuZn alloys during slow heating subsequent to deformation at cryogenic temperatures.

J. Freudenberger et al.: "Studies on recrystallization of single-phase copper alloys by resistance measurements", Acta Materialia 58 (2010) 2324-2329

Nobel Prize for H. K. Onnes in 1913

- In the beginning of the 20th century, it was an open question why free electrons (according to the Drude theory of metals with delocalized electrons) do not contribute to metal's heat capacity even though providing degrees of freedom of a gas.
- The temperature dependence of the electrical resistivity at low T was a key point to solve this problem. Three possibilities were basically considered: $\rho \to 0$ (1), $\rho \to \infty$ (rumored Einstein's favorite based on "freezing" the electrons at the atoms, 3) and $\rho \to \rho_0$ (2).

W. Buckel, R. Keiner: "Superconductivity", Weinheim: Wiley-VCH (2004)

Nobel Prize for H. K. Onnes in 1913

- Heike Kamerlingh Onnes was a physicist from The Netherlands. He was the first to liquefy He and, hence, able to cool to 4.2 K (liquid He) or 1.5 K (low pressure gas above liquid He). For his contributions to low temperature physics, he was awarded the Nobel prize in 1913.
- Apart from the discovery of superconductivity in Hg at slightly above 4.2 K, the investigations revealed that electrical resistivity of metals reaches a finite value at 0 K, the residual resistivity. The residual resistivity decreases with increasing purity suggesting that perfect metallic crystals exhibit no resistivity at 0 K.

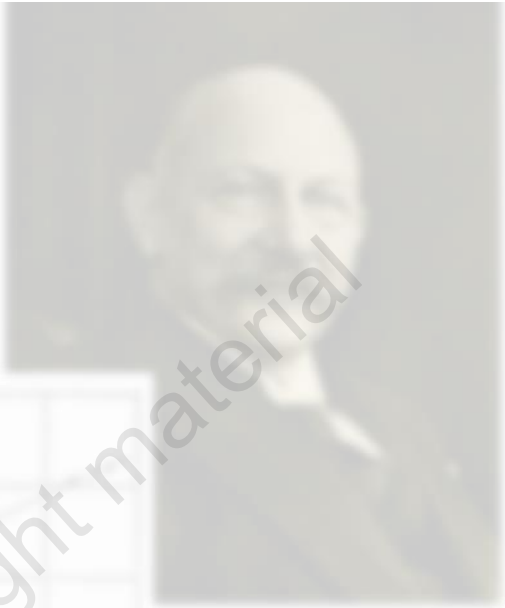

D. v. Delft & P. Kes: “The discovery of superconductivity”, Physics Today 63 (2010) 38-43
https://en.wikipedia.org/wiki/Heike_Kamerlingh_Onnes#/media/File:Kamerlingh_Onnes_signed.jpg

Nobel Prize for H. K. Onnes in 1913

- The vanishing resistivity of perfect crystals at 0 K is in (strong) disagreement with the Drude theory of metals (free electrons moving through the crystal of atoms should still collide with atoms).
- The appearance of quantum theory helped to overcome the contradiction: Electrons in metallic solids can be considered as waves in periodic potentials obeying Schrödinger‘s equation. The waves modulate with the periodic potential (Bloch theorem) and resistivity arises from deviations from the periodicity (defects, phonons, etc.) not from the atoms. Conducting electrons have large mean free-paths in pure metals in the order of several centimeters. An entire theory of metals, semi-metals, semiconductors and isolators became available by considering the diffraction of electron waves in reciprocal space and the according energy band gap between the diffracted (standing) waves.
- Furthermore, only a small fraction of electrons contributes to electrical conductivity (net occupied states in the direction of the electrical field and around the Fermi level). Hence, only a small fraction of electrons does contribute to specific heat capacity!

X-ray Diffraction (XRD)

- In case of **very small grain sizes** and **significant lattice strain**, **Bragg peaks broaden**.
- Both contributions can be separated for very simple assumptions: $\Delta(2\Theta)_S \approx 2\varepsilon \tan\Theta$ (strain) and $\Delta(2\Theta)_G \approx \frac{K\,\lambda}{D\cos\Theta}$ (grain size), with $\Delta(2\Theta)$ denoting the peak widths in 2Θ, ε the lattice strain, D the coherently scattering domain size, and K the Scherrer constant (between 0.89 and 0.94 depending on assumptions about peak shape, etc.).
- By considering the scattering vector $s = 2\sin\Theta\,/\lambda$, we get $\Delta s = \Delta(2\Theta)\cos\Theta\,/\lambda$ for the peak widths and:

$$\boldsymbol{\Delta s = \varepsilon\, s + \frac{K}{D}}$$

- The intercept $\frac{K}{D}$ gives an estimate for domain size (at $D \ll 1\ \mu\mathrm{m}$) and the slope an estimate for $\rho \propto \frac{\varepsilon^2}{b^2}$.
- Application of this simple version is often not possible since peak broadening is influenced also by other defects (like stacking faults) and (hkl)-depending broadening.

G. K. Williamson and W. H. Hall: “X-ray line broadening from filed Aluminium and Wolfram”, Acta Metallurgica 1 (1953) 22-31

X-ray Diffraction (XRD)

By plastic deformation, considerable peak broadening is caused. Nevertheless, it is not linearly depending on s.

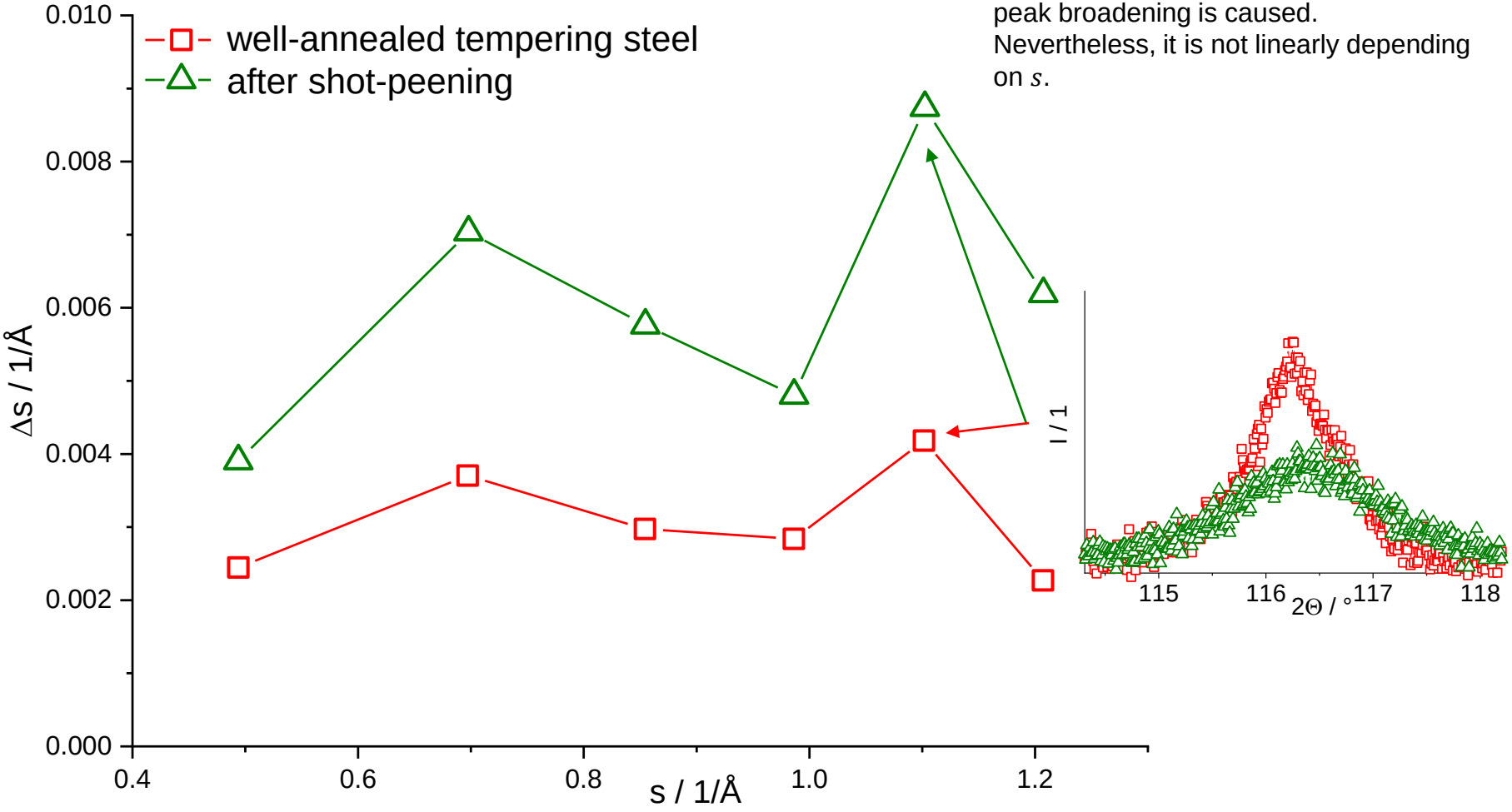

X-ray Diffraction (XRD)

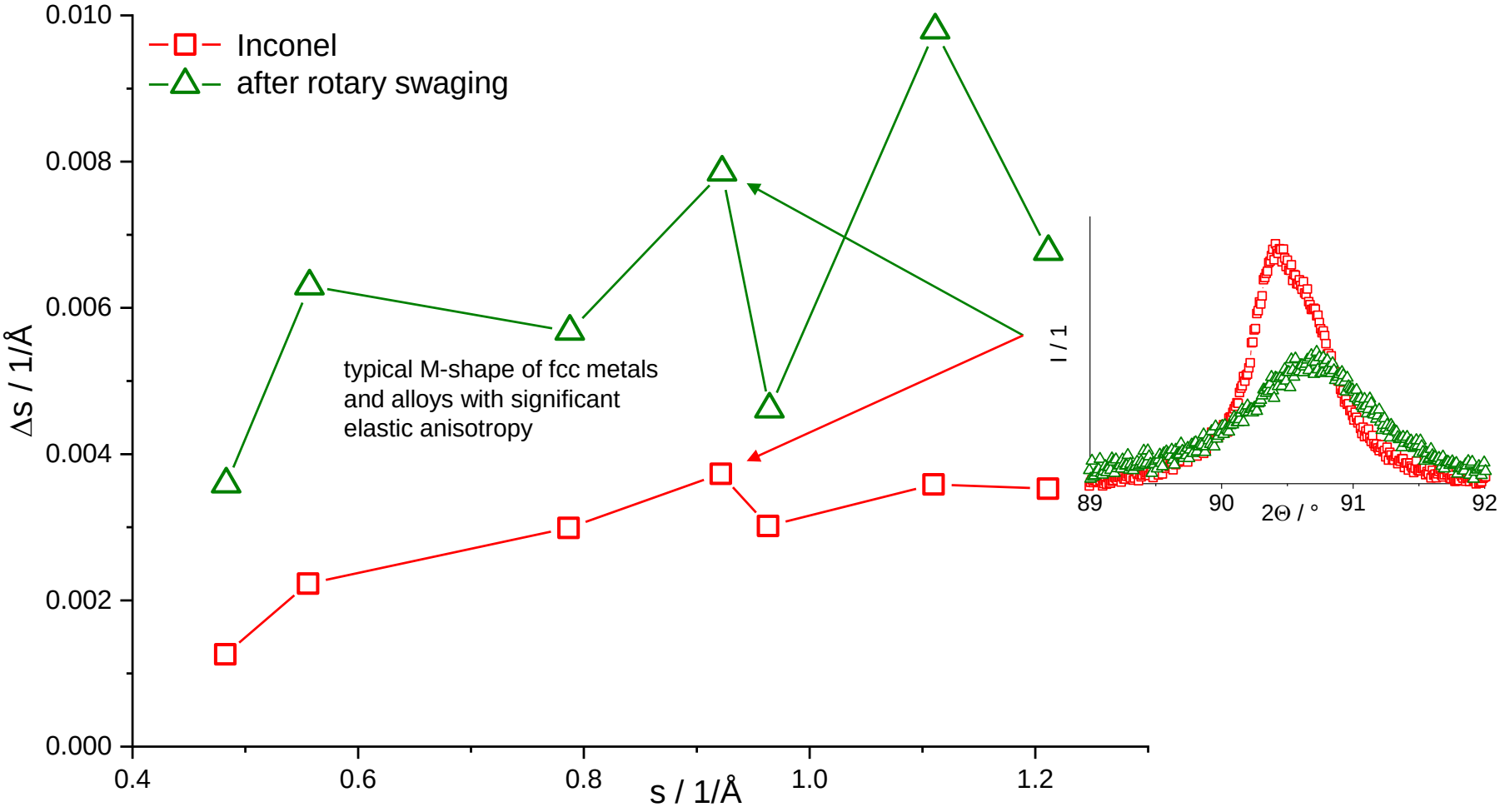

Summary

- **Direct evidence for dislocations is achieved by TEM**. There are different imaging methods with different lateral resolution possible TEM-BF, TEM-DF, HR-TEM, and „weak beam“-TEM-DF.
- **EBSD provides indirect qualitative and quantitative evidence for dislocations**.
- Dislocation densities can be evaluated under certain conditions by XRD, electrical resistivity and etch pit counting.